What Lies Beneath a Family of Aperiodic Monotilings

Iestyn Jowers[1] and Richard J. Moat[2]

[1]School of Engineering and Innovation, The Open University, UK; iestyn.jowers@open.ac.uk
[2]School of Engineering and Innovation, The Open University, UK; richard.moat@open.ac.uk

Abstract

In this paper the aperiodic monotilings discovered by David Smith and his collaborators are analysed according to the vertices of the tilings. It is shown that there are a variety of arrangements of vertices coincident with the monotiles, and when these are connected with straight lines (instead of polylines) sets of polygonal tiles are defined. Tilings based on these polygons suggest an underlying structure for the monotilings. These are presented, along with matching rules and edge modifications that give rise to alternative tilings, that are assumed to be aperiodic.

Introduction

The monotilings discovered by Smith et al. [2], are composed of single concave polygonal tiles and their reflections, and they offer an infinite family of aperiodic tilings of the plane. Using the definitions of Grünbaum and Shephard [1], a tile is an *n*-gon if it is polygonal with *n corners* and *n sides*, and each of the monotiles discovered by Smith et al. (with the exception of the chevron and the comet tiles) can be defined as a 13-gon, with thirteen corners and thirteen sides. This is illustrated by the seven tiles in Figure 1, which are members of the infinite family of tiles, defined by the changing relative lengths, *a* and *b*, of the sides. Each tile is identified by a vector (*a*, *b*), that specifies the ratio of lengths *a*:*b*, and some are named according to the figurative shape of the tile. In the chevron and comet tiles, (0, 1) and (1, 0) respectively, either the length *a* or the length *b* is equal to zero, resulting in fewer corners and sides.

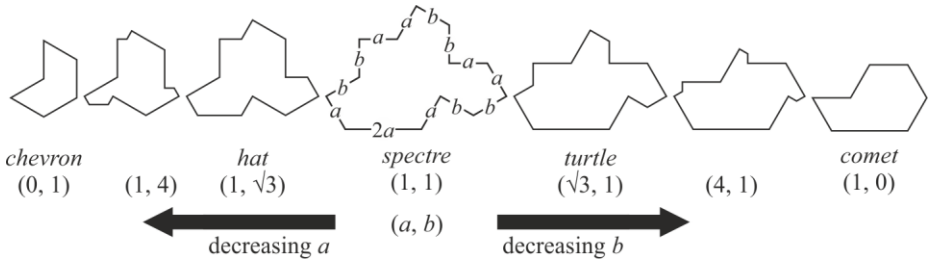

Figure 1: *An infinite family of convex polygonal tiles that result in aperiodic tilings.*

A tiling is an arrangement of tiles that covers the plane with no gaps or overlaps and, to avoid confusion, is described according to *vertices* (rather than corners) and *edges* (rather than sides) which connect the vertices. A vertex of a tiling is coincident with a corner if the corner is shared by three or more tiles. So a vertex has a valence of at least three (measured according to the number of edges it is coincident with). And, as a result, an edge of a tiling may be a polyline composed of multiple sides of a tile. A tiling is *edge-to-edge* if its vertices and edges coincide with the corners and sides of the tiles [1], but the aperiodic monotilings constructed from the tiles in Figure 1 are not edge-to-edge, since there are corners of the tiles that are not vertices of the tiling, and there are also vertices of the tiling that are not corners of the tiles. The consequences of this, with respect to the structure of the tilings, is considered in this paper, supporting an exploration of the family of aperiodic monotilings. This has resulted in the identification of sets of (mostly) convex polygonal tiles, which offer new insight into the underlying structure of the aperiodic monotilings. First this result is established for tilings of the hat tile, (1, √3), then it is shown how it applies to other members of the infinite family of aperiodic tilings.

Structure of the Hat Monotiling

A patch of the aperiodic monotiling based on the hat tile is illustrated in Figure 2a, with reflected tiles identified in grey, and the vertices of the tiling labelled with circular marks. The tiling is not edge-to edge because not all of the corners of the tiles are identified as vertices, and for some of the tiles, there is a vertex coincident with a midpoint of the side of length 2*a* (as shown in Figure 1). Due to the geometry of the hat tile (which has convex or concave angles only of 90° or 120°) the valence of the vertices is either three or four: it is three when three corners with angles of 120° meet, or when two corners of 90° meet at the midpoint of a side, with an angle of 180°; it is four when four corners with angles of 90° meet. In total, there are eleven arrangements of vertices coincident with the corners of the hat tile, and these are shown in Figure 2b. This set of eleven labelled tiles offers variations of the monotile, and can be used to explore the structure of the tiling.

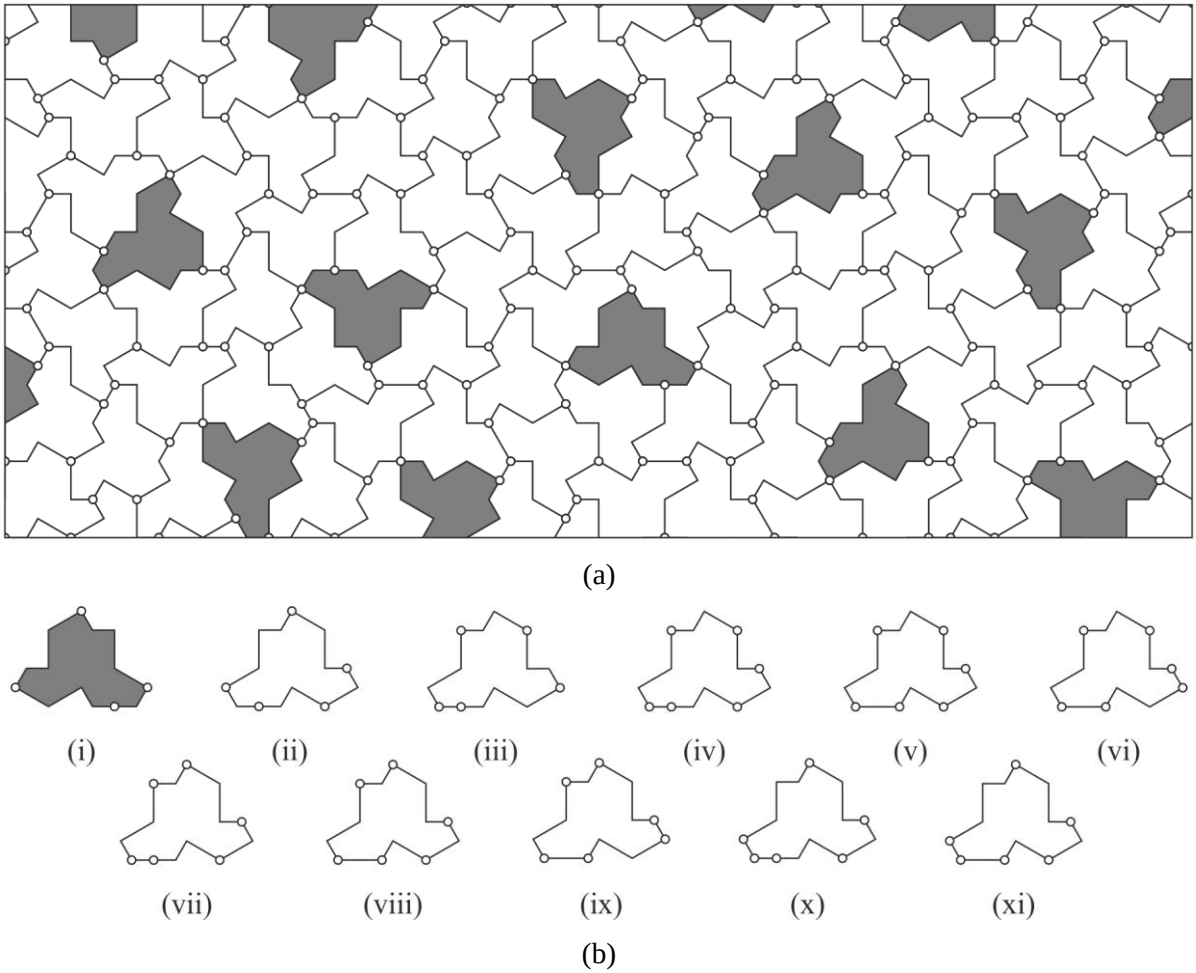

Figure 2: *Vertices of the hat monotiling: (a) a patch of the tiling, with vertices labelled by circular mark; (b) eleven arrangements of vertices coincident with corners of the hat tile.*

In the hat monotiling, the distribution of the eleven labelled tiles is not even. This is perhaps to be expected, since the reflected tiles, which account for approximately $\frac{1}{7}^{\text{th}}$ of the tiles, are all coincident with only one arrangement of vertices, as shown in Figure 2b-i, so there will necessarily be more of these than some of the other labelled tiles. Also, the labelled tiles in Figure 2b-ii and Figure 2b-iii are always and only adjacent to the reflected tiles, so they also each account for approximately $\frac{1}{7}^{\text{th}}$ of the tiles. The most common

arrangement of vertices coincident with a tile is that shown in Figure 2b-viii, which accounts for approximately ⅕th of the tiles, and is often adjacent to the reflected tile, but is also found elsewhere in the monotiling. The least common arrangement of vertices are those shown in Figure 2b-ix and Figure 2b-x, which each account for approximately only 1/50th of the tiles.

The distribution of vertices also gives rise to variations of the metatiles identified in the analysis of the hat tiling presented by Smith et al. [2] and used to reveal its underlying aperiodic order. For example, Figure 3 shows how the labelled tiles from Figure 2b are clustered according to the metatiles. The *H* metatile is a non-regular hexagon defined according to four tiles and is coincident with two arrangements of vertices, as shown in Figure 3a. It is always composed of tiles with the arrangement of vertices shown in Figure 2b-i, Figure 2b-ii and Figure 2b-iii and, as shown in Figure 3a-i and Figure 3a-ii respectively, either the arrangement shown in Figure 2b-x (approximately ⅐th of the *H* metatiles) or the arrangement shown in Figure 2b-xi (approximately ⅙th of the *H* metatiles). The *T* metatile is an equilateral triangle defined according to a single tile, and is coincident with just one arrangement of vertices, as shown in Figure 3b. It is always composed of the tile with the arrangement of vertices shown in Figure 2b-ix. The *P* metatile is a parallelogram defined according to two tiles, and is also coincident with just one arrangement of vertices, as shown in Figure 3c. It is always composed of tiles with the arrangement of vertices shown in Figure 2b-vi and Figure 2b-viii. The *F* metatile is a pentagonal triskelion leg defined according to two tiles, and is coincident with three arrangements of vertices, shown in Figure 3d, all of which include a key vertex, highlighted in red, which is used by Smith et al. [2] to construct supertiles. As shown in Figure 3d-i, Figure 3d-ii and Figure 3d-iii respectively, it is either composed of tiles with the arrangement of vertices shown in Figure 2b-iv and Figure 2b-vii (approximately ¼er of the *F* metatiles), or tiles with the arrangement shown in Figure 2b-iv and Figure 2b-viii (approximately 1/10th of the *F* metatiles), or tiles with the arrangement shown in Figure 2b-v and Figure 2b-viii (approximately ⅔rds of the *F* metatiles).

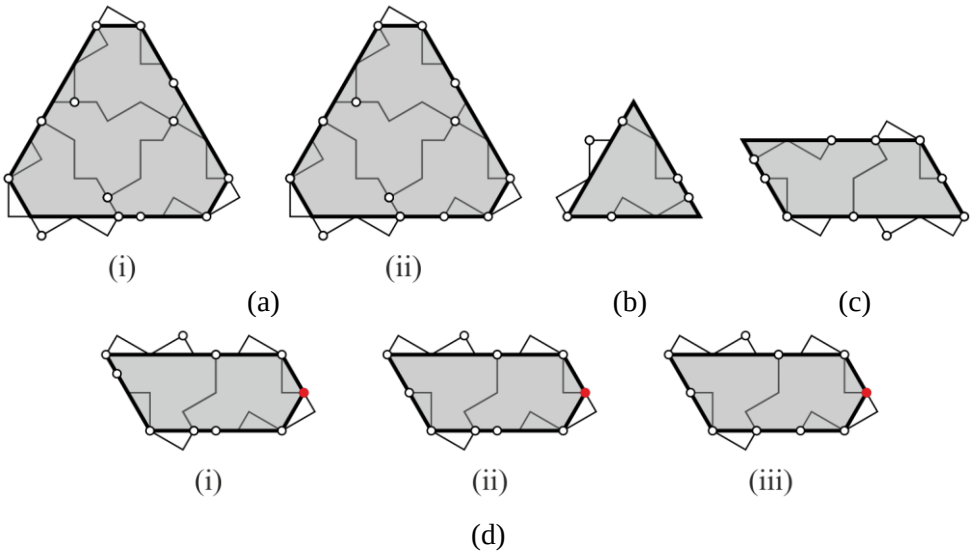

Figure 3: *Vertices of the hat metatiles: (a) two arrangements of the* H metatile*; (b) the* T *metatile; (c) the* P *metatile; (d) three arrangements of the* F *metatile, with key vertex highlighted.*

Discovering an Underlying Structure of the Hat Monotiling

Further insight into the underlying structure of the hat monotiling can be gained by using the vertices to reconstruct the tiling according to alternative sets of tiles. One such reconstruction is shown in Figure 4. Figure 4a shows a set of eight convex polygonal tiles that are constructed from the labelled tiles in Figure 2b by connecting the vertices with linear sides. Connecting the vertices coincident with the reflected tile (Figure 2b-i) results in a quadrilateral, and connecting vertices in the arrangement shown in Figure 2b-ix

results in a non-regular hexagon. For all other arrangements, connecting the vertices, results in non-regular pentagons. Due to the colinear alignment of some of the vertices, some pairs of arrangements (specifically those shown in Figure 2b-iv and Figure 2b-v; Figure 2b-vii and Figure 2b-viii; and Figure 2b-x and Figure 2b-xi) result in identical pentagons, and these are not repeated in Figure 4a.

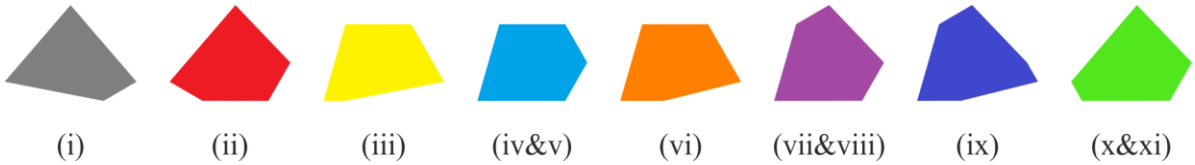

(a)

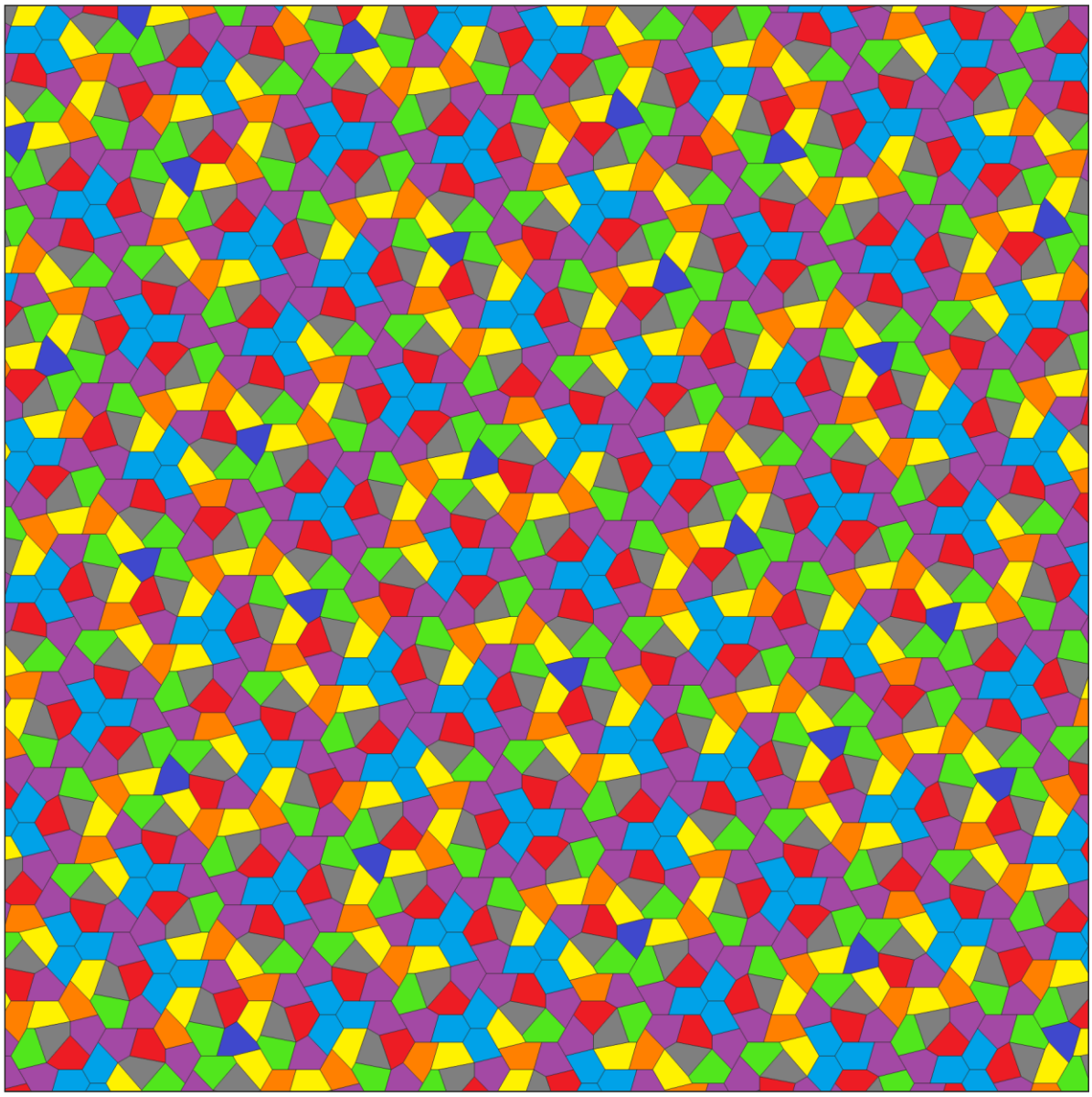

(b)

Figure 4: *Underlying structure of the hat monotiling: (a) set of eight convex polygons that result from connecting vertices of the monotiling; (b) a tiling of the polygons, equivalent to the hat monotiling.*

Figure 4b shows a patch of tiling that results from replacing the concave hat tiles with corresponding convex polygons from Figure 4a, coloured to make the distribution of the eight polygons visually apparent. The distribution of the polygons corresponds with the distribution of the labelled tiles in Figure 2a, but with the duplicated tiles merged as either light blue, purple or green polygons. Grey polygons (which correspond to the reflected hat tile) always have a neighbourhood consisting of red, green, yellow, and purple polygons. Dark blue tiles (which correspond to the *T* metatile) always have a neighbourhood consisting of red, green and yellow tiles. Light blue polygons always group in threes, forming a Y, the centre of which corresponds to the key vertices of the metatiles/supertiles. Yellow and orange tiles form oscillating worm-like chains. These patterns (and others) repeat throughout the tiling, but without translational symmetry and, since the arrangement of polygons is unchanged from the hat monotiling, the tiling is assumed to retain the aperiodic order of the monotiling. Replacement of the polyline sides of the hat tile with straight lines means that the edges of the tiling are now all linear, but it is still not edge-to-edge, because although all corners of the tiles are coincident with vertices of the tiling, there are also vertices not coincident with corners; these can be found on sides of the light blue, orange, purple and green polygons.

By analysing the arrangement of polygons in Figure 4b matching rules on the sides can be identified to specify how the tiles are combined in the tiling. These are shown in Figure 5, using the six labels α, β, γ, δ, ε, and ζ, and barred labels $\overline{\alpha}$, $\overline{\beta}$, $\overline{\gamma}$, $\overline{\delta}$, $\overline{\varepsilon}$, and $\overline{\zeta}$. In the tiling, sides with a label are always coincident with sides with the corresponding barred label, so only tiles with sides with matching label and barred label (for example α and $\overline{\alpha}$) can be adjacent. Comparing Figure 5 to Figure 4a, there are three additional tiles, because although the arrangement of vertices shown in Figure 2b-iv and Figure 2b-v, Figure 2b-vii and Figure 2b-viii, and Figure 2b-x and Figure 2b-xi, result in polygons with the same geometry, the matching rules for the pairs of tiles are different. To make the difference clear, circular labels are included in Figure 5 to show the arrangements of vertices of the tiling that are coincident with the polygonal tiles.

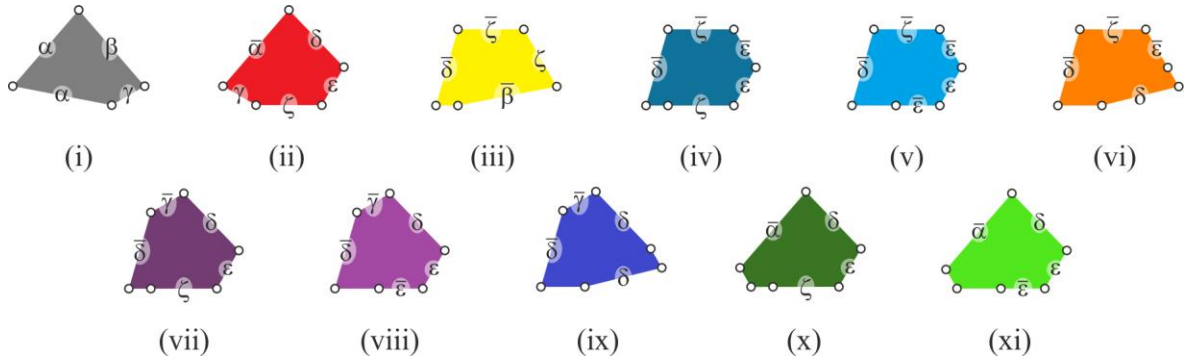

Figure 5: *Matching rules for the polygonal tiles in Figure 4.*

Using the matching rules in Figure 5 it is also possible to recreate the hat monotiling by replacing labels with edge modifications. The modifications required to achieve this are shown in Figure 6a, which shows six polylines, labelled α, β γ, δ, ε, and ζ, corresponding to the labelled sides in Figure 5. Unlabeled lines do not require modification. Vertices, corresponding with those on the tiles are also included in Figure 6 to show how the polylines align with the sides of the polygons. The shading in Figure 6a indicates which side of the polyline is inside the tile, and for barred labels, the inside is on the opposite side of the polyline. Applying the edge modifications in Figure 6a to the polygon in Figure 5-i will recreate the reflected hat tile and applying them to the other ten polygons, in Figure 5-ii to Figure 5-xi, will recreate the hat tile. So, applying the edge modifications to the tiling in Figure 4b, will recreate the hat monotiling. This shows that the hat monotiling can be reconstructed as a tiling of a set of eleven convex polygons, but with their edges modified such that they all have identical (or reflected) geometry.

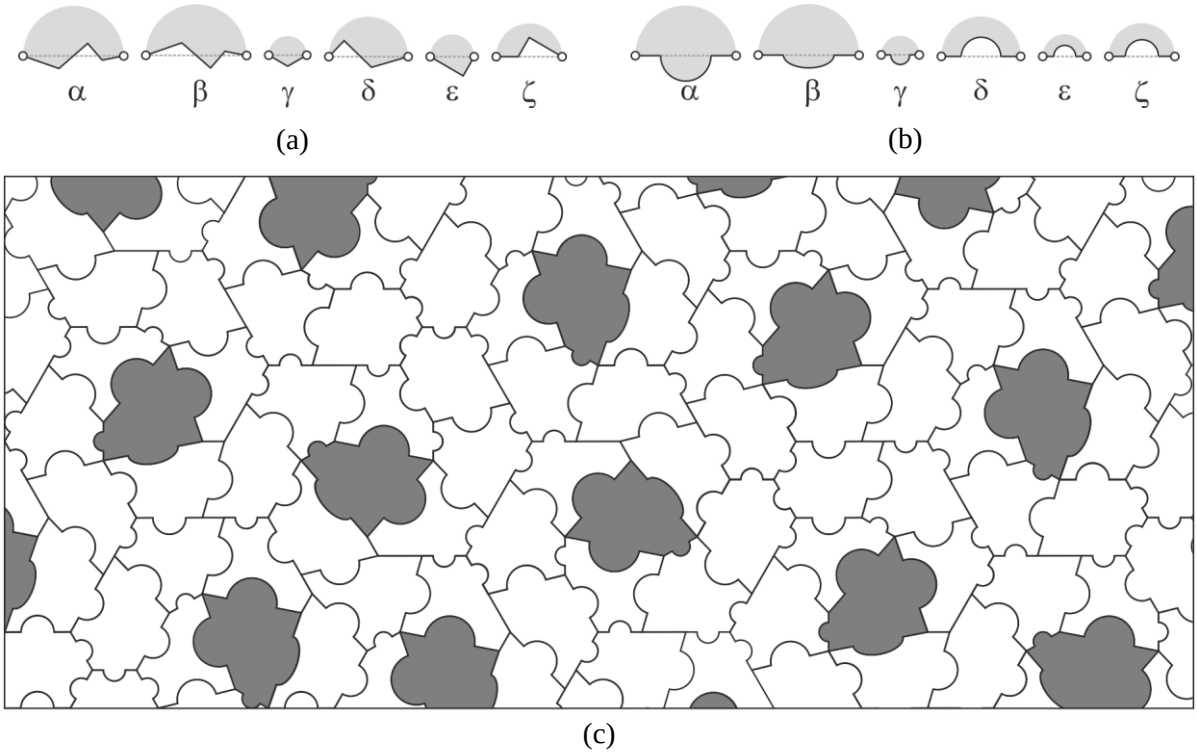

Figure 6: *Modifying the edges of the tiling: (a) edge modifications that recreate the hat monotiling; (b) alternative edge modifications; (c) a patch of tiling equivalent to the hat monotiling.*

This method of recreating the hat monotiling offers opportunities to design new tilings with aperiodic order, by changing the edge modifications; Figure 6 shows an example. In Figure 6b, an alternative set of edge modifications is shown, and these can be applied to the polygons as specified in Figure 5. Figure 6c shows the result of applying these alternative edge modifications to the patch of tiling from Figure 2a. The pattern lacks the sophistication and intrigue of a monotiling, being instead composed of a set of eleven jigsaw-like tiles. But the arrangement of the different tiles gives insight into the underlying structure of the monotiling, and since the arrangement of tiles is unchanged the tiling is assumed to retain the aperiodic order of the monotiling.

Discovering Underlying Structures of the Family of Aperiodic Monotilings

The same analysis can be applied to the other monotilings discovered by Smith et al. [2], offering reconstructions of each of the tilings according to sets of (mostly) convex polygons. The sets of polygonal tiles that result from connecting the vertices of seven of the monotilings is shown in Figure 7. The monotilings of the chevron and comet each have repeated tiles. Analysis of the aperiodic chevron tiling results in three distinct convex polygons: an equilateral triangle; a quadrilateral (a kite); and a non-regular pentagon. Analysis of the aperiodic comet tiling results in four distinct convex polygons: a rhombus; a non-regular pentagon; and two non-regular hexagons. This is due to either the length a or the length b (see Figure 1) being equal to zero, causing vertices to merge and resulting in fewer possible arrangements of the vertices. And, as shown in Figure 4, due to the colinear alignment of some of the vertices analysis of the hat monotiling results in eight distinct convex polygons: a quadrilateral, a non-regular hexagon, and six non-regular pentagons. For all other monotilings, defined by the changing relative lengths, a and b, of the sides of the tiles, there are eleven distinct polygons: a quadrilateral, two non-regular pentagons, and eight non-regular hexagons. These are mostly convex, although there is some concavity when the ratio b/a is greater than $\sqrt{3}$, with a not equal to 0, as shown in the polygons that result from analysis of the (1, 4) monotiling.

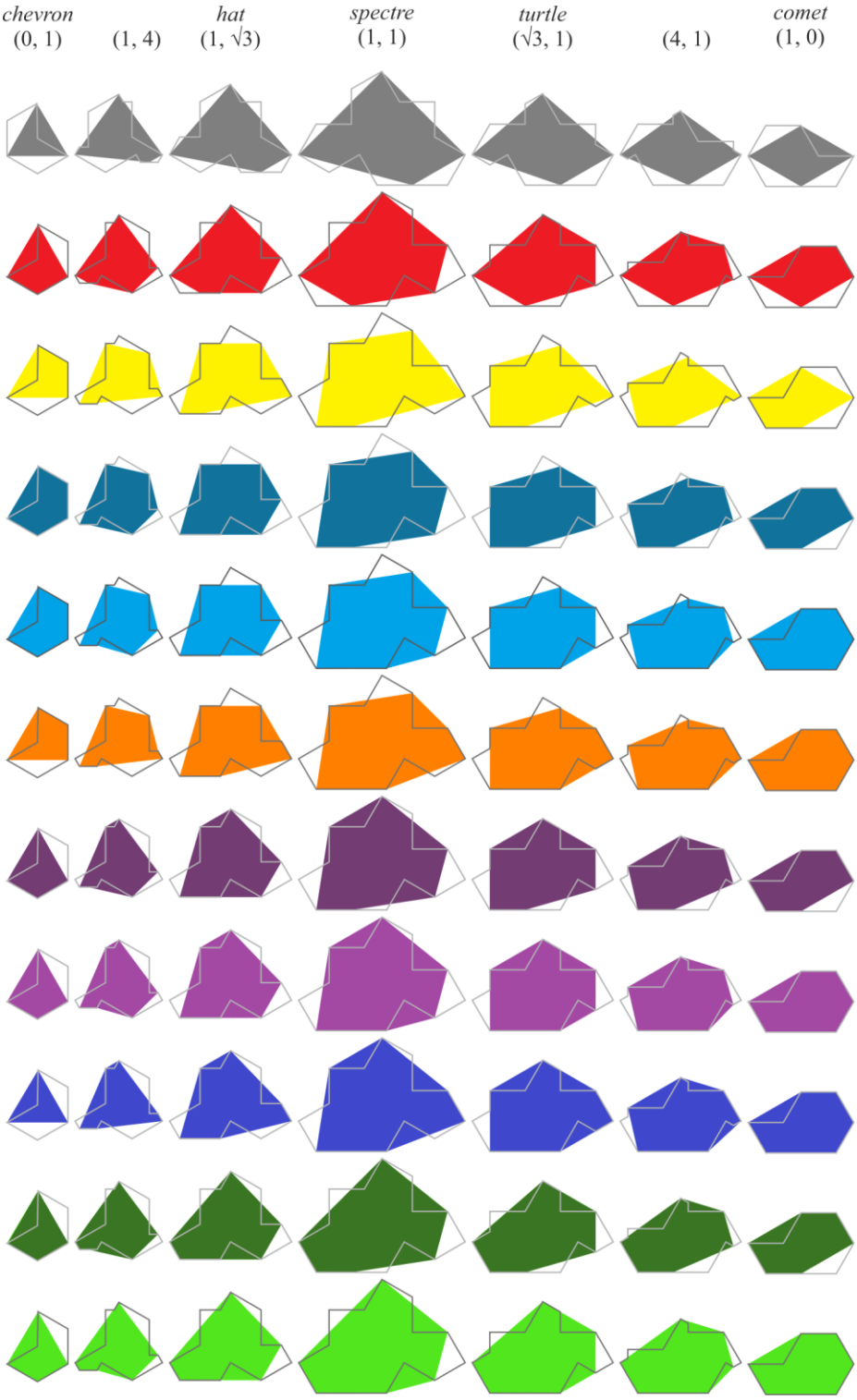

Figure 7: *Sets of polygonal tiles that result from connecting vertices of the monotilings.*

The sets of tiles in Figure 7 can be used to create new tilings, using matching rules corresponding to those in Figure 5, and such tilings will give insight into the underlying structure of the different monotilings. For example, Figure 8a, shows a patch of the tiling that results from replacing the chevron tiles with corresponding convex polygons from Figure 7. Identical polygons are coloured the same, so this tiling

includes only three polygons. Figure 8b shows a patch of the tiling that results from replacing the spectre tiles. Figure 8c shows a patch of the tiling that results from replacing the comet tiles. Again, identical polygons are coloured the same, so this tiling includes only four polygons. In each of these tilings the arrangement of polygons is unchanged from the corresponding monotiling, and patterns of tiles repeat without translational symmetry, so the tilings are assumed to retain the aperiodic order of the monotilings. And, as with the tiling in Figure 4b, edge modifications can be applied to these tilings to recreate the corresponding monotiling, or alternatively to to design new tilings with aperiodic order.

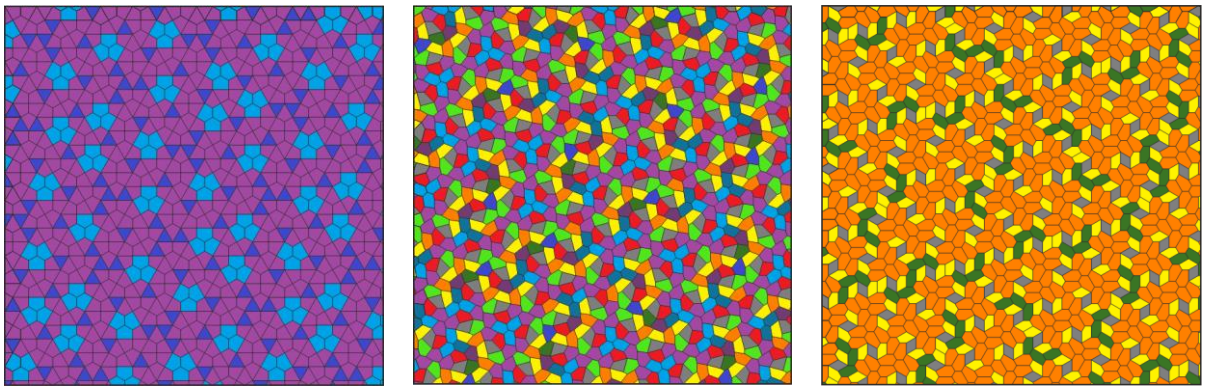

(a) (b) (c)

Figure 8: *Tiling of polygons equivalent to: (a) the chevron monotiling; (b) the spectre monotiling; (c) the comet monotiling.*

Summary and Conclusions

This paper has presented an exploration of the family of aperiodic monotilings discovered by Smith et al. [2], by analysing the configurations of the vertices of the tilings coincident with corners of the concave monotiles. This analysis has resulted in the identification of sets of (mostly) convex polygons that offer aperiodic tilings of the plane, and that are consistent with the metatiles introduced by Smith et al. [2] to reveal the underlying aperiodic order of the family of monotilings. It has also resulted in the discovery of new sets of tilings, assumed to be aperiodic. Firstly, there are the tilings of the polygons, which can result from connecting vertices of the monotilings with straight lines. They are infinite in number, corresponding to the number of monotilings discovered by Smith et al. [2], and examples are shown in Figure 4b and Figure 8, coloured to highlight the distribution of polygons. These offer a new interpretation of the aperiodic monotilings and give new insight into their underlying structure. Also, each of the polygonal tilings gives rise to uncountable variation via edge modification, using the matching rules in Figure 5. Two examples of edge modifications are shown in Figure 6, one to recreate the hat tiling, and one to create a simple jigsaw-like pattern. These suggest a potential to produce creative reconstructions of the monotilings with modified edges, perhaps even resulting in repeating Escher-like figures and forms.

Acknowledgements

Results reported in the paper were based on analysis of tilings generated using Craig Kaplan's interactive application [3].

References

[1] B. Grünbaum and G. C. Shephard. *Tilings and patterns: second edition*. Dover Publications, 2016.

[2] D. Smith, J. S. Myers, C. S, Kaplan, and C. Goodman-Strauss, C. "An aperiodic monotile." *Combinatorial Theory*, 4(1), 2024. https://doi.org/10.5070/C64163843

[3] Interactive tiling application, https://cs.uwaterloo.ca/~csk/hat/h7h8.html (accessed January 2025).